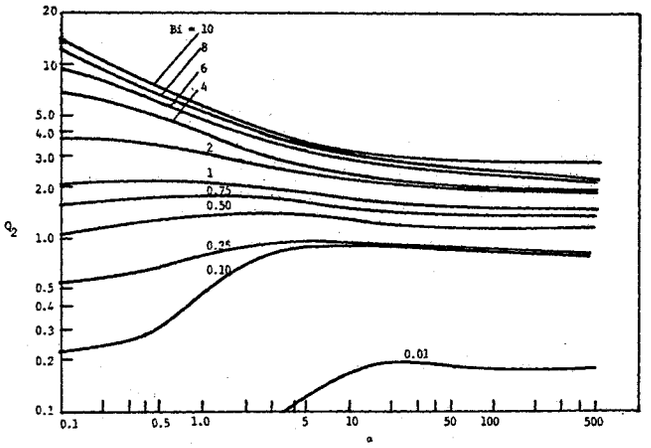

Fig. 3 Two-dimensional heat transfer rate in a straight triangular fin.

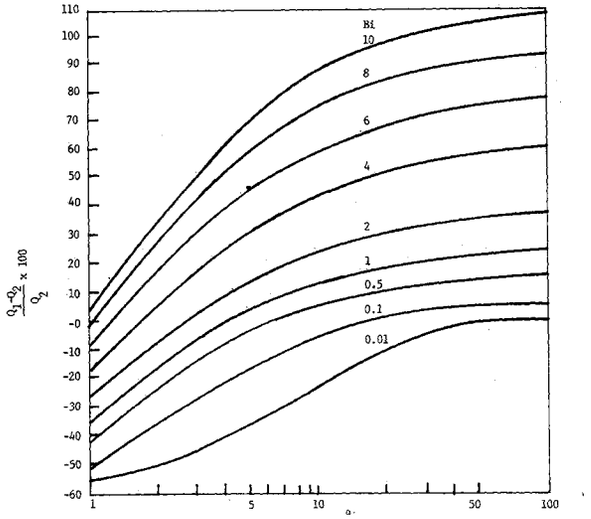

Fig. 4 Error in heat transfer rate in a triangular fin.

go beyond $x = 10$, I_0, and I_1 for certain combinations of α and Bi had to be evaluated from their series expansions. The percent error in heat transfer rate is plotted against α for various values of Bi in Fig. 4. It shows that the error can be positive or negative depending on the values of α and Bi. The error ranges from -55% to $+110\%$. It is interesting to note that the criterion of $Bi \ll 1$ generally accepted for the validity of one-dimensional assumption in a rectangular fin fails in the case of the triangular fin. For example, if the fin is thick and short, say $\alpha = 1$, the error is about -55% even when $Bi = 0.01$. On the other hand, the same fin can be treated as one-dimensional (with an error $+7\%$) at $Bi = 10$. Thus, it is not possible to establish a validity criterion for a triangular fin in terms of Bi number alone. It is the combination of α and Bi that dictate whether or not the one-dimensional assumption is valid. Table 2 shows the combinations for which the one-dimensional assumption will result in negligible error.

When using the results of this investigation, it is important to recognize the limitations of the analysis. One limitation is the assumption of a constant heat transfer coefficient, h. Studies by Stachiewicz,[7] Unal,[8] and Look[9] have shown that h can vary significantly along the convecting surface. Another limitation is that the base temperature T_b is spatially uniform. It is known from the works of Sparrow and Hennecke,[10] Klett and McCulloch,[11] and Look[12] that the fin base temperature is depressed and becomes nonuniform as a result of the thermal interaction between the fin and the primary surface to which it is attached. In view of these and other limitations that characterize many fin studies, the results of the present investigation, like any other investigation, must be used with caution.

References

[1]Lau, W., and Tan, C. W., "Errors in One-Dimensional Heat Transfer Analysis in Straight and Annular Fins," *ASME Journal of Heat Transfer*, Vol. 95, 1973, pp. 549–551.

[2]Irey, R. K., "Errors in the One-Dimensional Fin Solution," *ASME Journal of Heat Transfer*, Vol. 90, 1968, pp. 175–176.

[3]Levitsky, M., "The Criterion for Validity of the Fin Approximation," *International Journal of Heat and Mass Transfer*, Vol. 15, 1972, pp. 1960–1963.

[4]Sfeir, A. A., "The Heat Balance Integral in Steady-State Conduction," *ASME Journal of Heat Transfer*, Vol. 98, 1976, pp. 466–470.

[5]Burmeister, L. C., "Triangular Fin Performance by the Heat Balance Integral Method," *ASME Journal of Heat Transfer*, Vol. 101, 1979, pp. 562–564.

[6]Kraus, A. D., Extended Surface Heat Transfer, McGraw Hill, New York, 1972.

[7]Stachiewicz, J. W., "Effect of Variation of Local Film Coefficients on Fin Performance," *ASME Journal of Heat Transfer*, Vol. 91, 1969, pp. 21–26.

[8]Unal, H. C. "Temperature Distributions in Fin with Uniform and Non-Uniform Heat Transfer Coefficient," *International Journal of Heat and Mass Transfer*, Vol. 30, 1987, pp. 1465–1467.

[9]Look, Jr., D. C., "Two-Dimensional Fin Performance: *Bi* (top surface) $\geq$ *Bi* (bottom surface)," *ASME Journal of Heat Transfer*, Vol. 110, 1988, pp. 780–782.

[10]Sparrow, E. M. and Hennecke, D. K., "Temperature Depression at the Base of the Fin," *ASME Journal of Heat Transfer*, Vol. 92, 1970, pp. 204–206.

[11]Klett, D. E., and McCulloch, J. W., "The Effect of Thermal Conductivity and Base Temperature Depression on Fin Effectiveness," *ASME Journal of Heat Transfer*, Vol. 94, 1972, pp. 333–334.

[12]Look, D. C., "Two-Dimensional Fin with Non-constant Root Temperature," *International Journal of Heat and Mass Transfer*, Vol. 32, 1989, pp. 977–980.

Entrance Heat Transfer in Isosceles and Right Triangular Ducts

R. Lakshminarayanan*
Ketema Inc., Dallas, Texas 75051
and
A. Haji-Sheikh†
University of Texas at Arlington, Arlington, Texas 76019

Introduction

HEAT transfer from isosceles and right triangular ducts to an incompressible fluid with constant physical properties is presented. The flow is laminar and hydrodynamically fully developed; however, it develops thermally with the walls maintained at a constant temperature. Axial conduction, viscous dissipation, flow work, and thermal energy generation within the fluid are neglected.

Heat transfer in noncircular ducts is of considerable importance in the design of compact heat exchangers. A Galerkin-based integral method is used to carry out the computations. A generalized procedure that results in a closed-form solution for noncircular ducts was reported earlier.[1] The data presented here are comprehensive and cover a wider range than those in Ref. 1.

Received March 21, 1990; revision received May 30, 1990; accepted for publication May 31, 1990. Copyright © 1990 by the American Institute of Aeronautics and Astronautics, Inc. All rights reserved.

*Applications Engineer, Heat Transfer Division, 2300 West Marshall.

†Professor, Mechanical Engineering Department. Member AIAA.

The fully developed velocity distribution is obtained independent of the energy equation because the physical properties do not depend on temperature. A simple and accurate method of solving the hydrodynamically fully developed velocity problem in ducts of noncircular cross section was reported by Haji-Sheikh et al.[2] The method also uses the Galerkin technique to solve Poisson's equation and to find the velocity distribution, as well as the friction factors, for a variety of ducts.

Description of Analysis

The dimensionless form of the energy equation in the absence of axial conduction is

$$\rho c_p u(y,z) \frac{\partial T}{\partial x} = \nabla \cdot (k \nabla T) \tag{1}$$

where T, ρ, c_p, k, and u are the temperature, density, specific heat, thermal conductivity, and local velocity, respectively. The coordinates (y,z) are in the cross section and x is the axial coordinate in the flow direction. The Laplace operator is for (y,z) coordinates (the axial conduction is neglected). The heated section of the pipe has a constant temperature. The unheated fluid entering the heated section is laminar and fully developed with uniform temperature. The solution of Eq. (1) can be expressed in terms of the Green's function. The solution of Eq. (1) using the Green's function solution for position-dependent ρc_p is given in Ref. 3. The procedure for this problem is the same, except that the position-dependent ρc_p is now replaced by $\rho c_p u(y,z)$. The Green's function and the Green's function solution method remain unchanged. The integral solution method[1] and the alternative Green's function solution[3] yield identical results.

The temperature data are used to calculate heat flux and subsequently the heat transfer coefficient.[1] The circumferentially averaged heat transfer coefficient h is obtained from the relation

$$dQ_w = hP\, dx(T_w - T_b) = \dot{m} c_p\, dT_b \tag{2}$$

where Q_w is heat transfer rate, P is perimeter, and $\dot{m}$ is mass flow rate. The lengthwise average, or mean, heat transfer coef-

Table 1 Local and mean Nusselt number data in entrance region of isoceles triangular ducts for various included angles, 2β

	$2\beta = 2.5$ deg		$2\beta = 5$ deg		$2\beta = 10$ deg		$2\beta = 20$ deg	
X	Nu	$\bar{N}u$	Nu	$\bar{N}u$	Nu	$\bar{N}u$	Nu	$\bar{N}u$
0.0001	24.051	156.753	22.951	131.523	23.587	75.720	22.868	54.044
0.0002	21.878	89.841	20.958	76.723	21.067	48.999	20.211	37.762
0.0004	18.597	54.989	17.918	48.035	17.439	34.061	16.577	28.003
0.0006	16.295	42.453	15.761	37.617	15.041	28.094	14.287	23.786
0.0008	14.625	35.694	14.187	31.947	13.392	24.613	12.755	21.208
0.0010	13.374	31.350	13.002	28.271	12.216	22.245	11.678	19.403
0.0020	10.067	21.399	9.847	19.719	9.399	16.392	9.146	14.784
0.0040	7.726	15.047	7.575	14.118	7.552	12.359	7.482	11.485
0.0060	6.666	12.413	6.541	11.748	6.601	10.587	6.582	9.991
0.0080	6.012	10.889	5.906	10.362	5.958	9.505	5.950	9.055
0.0100	5.560	9.866	5.468	9.424	5.495	8.747	5.480	8.385
0.0200	4.427	7.383	4.362	7.125	4.324	6.778	4.247	6.573
0.0400	3.499	5.642	3.460	5.487	3.463	5.303	3.389	5.158
0.0600	3.011	4.840	2.995	4.727	3.046	4.614	3.008	4.498
0.0800	2.709	4.342	2.710	4.256	2.789	4.187	2.779	4.095
0.1000	2.506	3.994	2.521	3.927	2.611	3.889	2.626	3.816
0.2000	2.051	3.114	2.098	3.097	2.178	3.122	2.287	3.118
0.4000	1.748	2.494	1.822	2.517	1.921	2.572	2.117	2.650
0.6000	1.607	2.220	1.697	2.263	1.824	2.337	2.073	2.463
0.8000	1.519	2.055	1.622	2.111	1.773	2.202	2.059	2.363
1.0000	1.457	1.941	1.573	2.008	1.744	2.113	2.054	2.302
2.0000	1.320	1.657	1.483	1.761	1.702	1.914	2.050	2.176
4.0000	1.266	1.471	1.462	1.615	1.696	1.806	2.050	2.113
6.0000	1.254	1.400	1.459	1.563	1.696	1.769	2.050	2.092
8.0000	1.251	1.363	1.459	1.537	1.696	1.751	2.050	2.081
	$2\beta = 30$ deg		$2\beta = 40$ deg		$2\beta = 50$ deg		$2\beta = 60$ deg	
0.0001	22.087	45.027	21.317	39.725	20.754	35.993	20.131	33.118
0.0002	19.523	32.886	18.892	29.888	18.260	27.722	17.431	25.916
0.0004	16.049	25.263	15.540	23.485	14.846	22.067	13.901	20.708
0.0006	13.881	21.804	13.423	20.458	12.730	19.281	11.834	18.066
0.0008	12.438	19.632	12.013	18.512	11.350	17.459	10.540	16.334
0.0010	11.427	18.086	11.026	17.108	10.398	16.137	9.668	15.083
0.0020	9.012	14.040	8.633	13.362	8.104	12.592	7.574	11.761
0.0040	7.266	11.030	6.834	10.485	6.401	9.858	5.993	9.213
0.0060	6.292	9.601	5.900	9.099	5.560	8.553	5.215	7.998
0.0080	5.638	8.687	5.315	8.221	5.036	7.735	4.735	7.238
0.0100	5.177	8.029	4.917	7.597	4.677	7.157	4.406	6.703
0.0200	4.089	6.279	3.954	5.975	3.772	5.654	3.567	5.311
0.0400	3.329	4.965	3.224	4.753	3.099	4.515	2.966	4.261
0.0600	2.971	4.354	2.902	4.184	2.824	3.992	2.734	3.786
0.0800	2.764	3.980	2.729	3.840	2.681	3.680	2.621	3.507
0.1000	2.633	3.723	2.623	3.606	2.599	3.471	2.562	3.323
0.2000	2.374	3.097	2.442	3.056	2.485	2.996	2.498	2.919
0.4000	2.285	2.706	2.407	2.736	2.475	2.736	2.495	2.707
0.6000	2.274	2.563	2.405	2.626	2.475	2.649	2.495	2.637
0.8000	2.272	2.491	2.405	2.571	2.475	2.606	2.495	2.601
1.0000	2.272	2.447	2.405	2.538	2.475	2.579	2.495	2.580
2.0000	2.271	2.359	2.405	2.471	2.475	2.527	2.495	2.538
4.0000	2.271	2.315	2.405	2.438	2.475	2.501	2.495	2.517

Table 1 Continued

	$2\beta = 90$ deg		$2\beta = 120$ deg		$2\beta = 150$ deg		$2\beta = 170$ deg	
0.00001	21.758	90.735	20.420	52.351	15.072	25.965	7.484	11.402
0.00002	20.994	56.053	18.530	35.893	12.261	19.720	5.703	8.937
0.00004	19.633	38.175	15.877	26.498	9.916	15.317	4.343	6.918
0.00006	18.463	31.794	14.152	22.651	8.729	13.303	3.788	5.957
0.00008	17.452	28.332	12.957	20.368	7.932	12.055	3.457	5.371
0.00010	16.574	26.066	12.079	18.794	7.325	11.167	3.217	4.963
0.00020	13.546	20.486	9.677	14.748	5.564	8.743	2.544	3.897
0.00040	10.658	16.192	7.629	11.632	4.275	6.770	2.054	3.075
0.00060	9.207	14.084	6.537	10.101	3.748	5.842	1.860	2.698
0.00080	8.284	12.742	5.835	9.116	3.426	5.276	1.745	2.473
0.00100	7.626	11.781	5.353	8.409	3.190	4.881	1.663	2.319
0.00200	5.918	9.207	4.217	6.544	2.546	3.850	1.457	1.930
0.00400	4.682	7.201	3.407	5.147	2.107	3.066	1.380	1.667
0.00600	4.121	6.259	3.007	4.494	1.937	2.715	1.374	1.570
0.00800	3.772	5.678	2.765	4.090	1.838	2.507	1.373	1.521
0.01000	3.525	5.271	2.606	3.808	1.771	2.366	1.373	1.491
0.02000	2.907	4.215	2.263	3.103	1.632	2.025	1.373	1.432
0.04000	2.538	3.448	2.087	2.628	1.601	1.817	1.373	1.403
0.06000	2.426	3.123	2.044	2.439	1.599	1.745	1.373	1.373
0.08000	2.384	2.943	2.032	2.339	1.599	1.708		
0.10000	2.368	2.829	2.029	2.277	1.599	1.686		
0.20000	2.357	2.594	2.028	2.152	1.599	1.643		
0.40000	2.357	2.475	2.028	2.090	1.599	1.599		
0.60000	2.357	2.436	2.028	2.069				
0.80000	2.357	2.416	2.028	2.059				
1.00000	2.357	2.404	2.028	2.053				
2.00000	2.357	2.380						
4.00000	2.357	2.357						

Table 2 Comparison of local and mean Nusselt numbers for a right-angled isosceles triangular duct

	Nusselt number, Nu		Mean Nusselt number, $\bar{N}u$	
X	Results	Ref. 4	Results	Ref. 4
0.000686	8.7651	—	13.4424	—
0.001373	6.7823	—	10.5305	—
0.003431	4.9206	4.74	7.5990	6.33
0.003813	4.7546	4.57	7.3227	6.17
0.004289	4.5783	4.40	7.0273	6.00
0.004902	4.3892	4.21	6.7089	5.78
0.005719	4.1831	4.01	6.3623	5.52
0.008579	3.6928	3.50	5.5468	4.91
0.011440	3.3864	3.20	5.0424	4.52
0.013730	3.2119	3.05	4.7512	4.28
0.017160	3.0216	2.90	4.4232	4.01
0.022880	2.8162	2.70	4.0449	3.70
0.034310	2.5994	2.53	3.5945	3.33
0.068630	2.4028	2.40	3.0338	2.87
0.137300	2.3591	—	2.7025	—

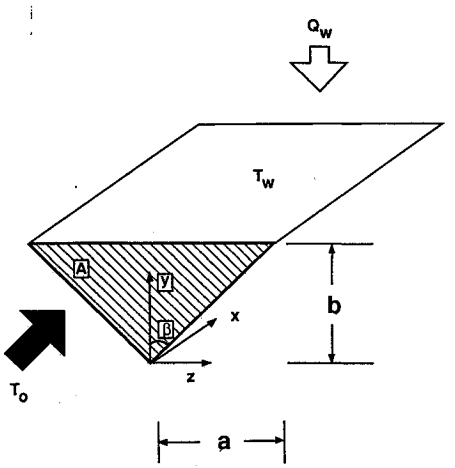

Fig. 1 Geometry of an isosceles triangular duct.

ficient $\bar{h}$ is related to the circumferential average heat transfer coefficient h through the relation

$$\bar{h} = \frac{1}{x}\int_0^x h\, dx \tag{3}$$

The circumferential averaged Nusselt number is $Nu = hD_e/k$ and the lengthwise averaged Nusselt number is $\bar{N}u = \bar{h}D_e/k$, where $D_e = 4A/P$ is the hydraulic diameter.

Numerical Examples

Two examples are presented: flow in an isosceles triangular duct and flow in a right triangular duct. The difference between the two solutions is the selection of the basis functions. Polynomial basis functions are used because all integrations leading to the solutions have exact values.[1] The basis functions are presented in the following sections.

Isosceles Triangular Ducts

The geometry of an isosceles triangular duct is shown in Fig. 1. The corresponding basis functions $f_j(\bar{y},\bar{z})$, when $\bar{b} = b/a$, $\bar{y} = y/a$, and $\bar{z} = z/a$, are

$$\phi(\bar{y},\bar{z}) = [(\bar{y})^2 - (\bar{b}\bar{z})^2](\bar{y} - \bar{b}) \tag{4}$$

and

$$f_j(\bar{y},\bar{z}) = \phi(\bar{y},\bar{z})P_{mj}(\bar{y})P_{nj}(\bar{z}), \qquad j = 1, 2, 3, \ldots, N \tag{5}$$

where the polynomials are $P_{mj}(\bar{y}) = (\bar{y})^{mj}$ and $P_{nj}(\bar{z}) = (\bar{z})^{nj}$. Because of the symmetry, the terms with odd exponents on z in Eq. (5) can be omitted. The characteristic length is equal to one-half of the base a (Fig. 1).

The Nusselt number data in the entrance region of various isosceles triangular ducts are presented in Table 1. Table 1 and all subsequent tables contain both the local and mean Nusselt numbers for different angles β and different dimensionless axial distance $X = (xD_e)/(a^2RePr)$. The Reynolds number is $Re = \bar{u}D_e/\nu$, and the Prandtl number is $Pr = \nu/\alpha$, where α and ν are thermal diffusivity and kinematic viscosity, and $\bar{u}$ is the mean velocity. The data were obtained by using 25 terms in the

Table 3 Local and mean Nusselt number data in entrance region of right triangular ducts for various included angles, β

	$\beta = 2.5$ deg		$\beta = 5$ deg		$\beta = 10$ deg		$\beta = 15$ deg		$\beta = 20$ deg	
X	Nu	$\bar{Nu}$	Nu	$\bar{Nu}$	Nu	$\bar{Nu}$	Nu	$\bar{Nu}$	Nu	$\bar{Nu}$
0.00008	20.321	63.132	19.565	55.836	18.206	44.578	17.146	37.961	16.355	33.598
0.00010	19.077	54.443	18.462	48.469	17.305	39.212	16.373	33.720	15.664	30.079
0.00020	14.834	35.587	14.542	32.393	13.949	27.351	13.413	24.251	12.975	22.152
0.00040	10.963	24.095	10.754	22.382	10.435	19.653	10.166	17.918	9.932	16.711
0.00060	9.172	19.388	8.980	18.180	8.723	16.266	8.533	15.034	8.376	14.166
0.00080	8.128	16.694	7.956	15.742	7.736	14.247	7.589	13.282	7.476	12.597
0.00100	7.448	14.908	7.291	14.114	7.099	12.877	6.985	12.079	6.905	11.512
0.00200	5.937	10.726	5.814	10.261	5.696	9.568	5.664	9.137	5.648	8.834
0.00400	4.829	8.019	4.735	7.732	4.665	7.341	4.658	7.118	4.625	6.957
0.00600	4.209	6.845	4.139	6.626	4.096	6.347	4.086	6.196	4.028	6.073
0.00800	3.786	6.130	3.737	5.951	3.718	5.734	3.706	5.618	3.637	5.509
0.01000	3.475	5.629	3.444	5.478	3.445	5.302	3.435	5.207	3.365	5.106
0.02000	2.671	4.316	2.687	4.239	2.747	4.169	2.755	4.121	2.730	4.046
0.04000	2.165	3.342	2.204	3.318	2.292	3.322	2.326	3.309	2.356	3.275
0.06000	1.961	2.912	2.014	2.912	2.111	2.945	2.162	2.951	2.216	2.943
0.08000	1.835	2.657	1.900	2.672	2.002	2.722	2.070	2.741	2.144	2.751
0.10000	1.746	2.484	1.820	2.509	1.927	2.570	2.012	2.601	2.104	2.625
0.20000	1.504	2.045	1.614	2.104	1.764	2.198	1.916	2.275	2.052	2.347
0.40000	1.336	1.724	1.488	1.820	1.710	1.963	1.898	2.089	2.046	2.197
0.60000	1.289	1.585	1.460	1.704	1.702	1.877	1.896	2.025	2.046	2.147
0.80000	1.271	1.508	1.452	1.642	1.699	1.833	1.896	1.993	2.046	2.121
1.00000	1.262	1.460	1.449	1.603	1.698	1.806	1.896	1.973	2.046	2.106
2.00000	1.251	1.357	1.446	1.525	1.698	1.752	1.896	1.934	2.046	2.076
4.00000	1.250	1.304	1.446	1.486	1.698	1.725	1.896	1.896	2.046	2.046
0.00008	15.731	30.395	15.221	27.876	14.785	25.800	14.366	24.030	13.918	22.464
0.00010	15.095	27.398	14.616	25.284	14.185	23.536	13.746	22.035	13.248	20.687
0.00020	12.591	20.579	12.220	19.312	11.820	18.230	11.341	17.246	10.738	16.289
0.00040	9.704	15.778	9.444	14.990	9.115	14.266	8.693	13.546	8.169	12.778
0.00060	8.215	13.480	8.017	12.879	7.754	12.299	7.413	11.692	7.005	11.026
0.00080	7.359	12.048	7.202	11.553	6.983	11.058	6.698	10.525	6.359	9.933
0.00100	6.816	11.052	6.685	10.628	6.491	10.191	6.233	9.710	5.930	9.173
0.00200	5.592	8.574	5.466	8.302	5.269	7.990	5.023	7.627	4.753	7.218
0.00400	4.522	6.787	4.354	6.574	4.157	6.315	3.955	6.019	3.746	5.694
0.00600	3.906	5.921	3.754	5.725	3.605	5.494	3.461	5.240	3.306	4.963
0.00800	3.520	5.365	3.401	5.184	3.296	4.980	3.188	4.758	3.064	4.516
0.01000	3.266	4.969	3.179	4.804	3.101	4.622	3.013	4.425	2.907	4.209
0.02000	2.714	3.951	2.696	3.847	2.659	3.731	2.606	3.599	2.543	3.449
0.04000	2.382	3.233	2.394	3.180	2.397	3.114	2.394	3.034	2.383	2.943
0.06000	2.263	2.927	2.302	2.900	2.334	2.862	2.356	2.813	2.361	2.752
0.08000	2.211	2.754	2.270	2.746	2.317	2.728	2.348	2.697	2.358	2.653
0.10000	2.187	2.642	2.258	2.649	2.312	2.645	2.346	2.627	2.357	2.594
0.20000	2.164	2.406	2.249	2.450	2.310	2.478	2.345	2.486	2.357	2.476
0.40000	2.162	2.284	2.249	2.350	2.310	2.394	2.345	2.416	2.357	2.416
0.60000	2.162	2.243	2.249	2.316	2.310	2.366	2.345	2.392	2.357	2.396
0.80000	2.162	2.223	2.249	2.299	2.310	2.352	2.345	2.380	2.357	2.387
1.00000	2.162	2.211	2.249	2.289	2.310	2.343	2.345	2.373	2.357	2.381
2.00000	2.162	2.186	2.249	2.269	2.310	2.310	2.345	2.345	2.357	2.357
4.00000	2.162	2.162	2.249	2.249	2.310	2.310	2.345	2.345	2.357	2.357

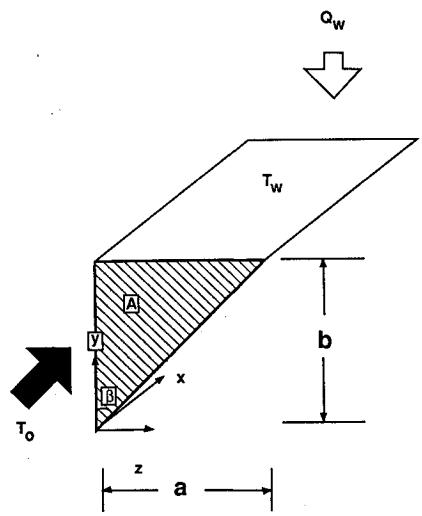

Fig. 2 Geometry of a right triangular duct.

finite-series approximation for both the velocity and the temperature profiles with the highest degree of the polynomial, in y or z, being limited to eight. A large number of terms is required for an accurate prediction in this region because the finite series converges slowly. However, during computations, it is observed that the matrix B (in Ref. 1) loses its structure while undergoing Cholesky decomposition for values of N greater than specific values. The values of N are 20 for $\beta < 5$ deg and 25 for $\beta > 5$ deg. Table 2 compares the local and mean Nusselt numbers for a right-angled isosceles triangular duct with the data reported in Ref. 4. The data in Table 1 are accurate and generally agree with the numerical data of Wilbulswas.[4] All data presented here are from Ref. 5. The computation time is negligibly small on minicomputers or personal computers.

Right Triangular Passages

The geometry of a right triangular duct is shown in Fig. 2. The basis functions $f_j(\bar{y},\bar{z})$, when $\bar{b} = b/a$, $\bar{y} = y/a$, and $\bar{z} = z/a$, are

$$\phi(\bar{y},\bar{z}) = \bar{z}(\bar{y} - \bar{b})(\bar{y} - \bar{b}\bar{z}) \tag{6}$$

and

$$f_j(\bar{y},\bar{z}) = \phi(\bar{y},\bar{z})P_{mj}(\bar{y})P_{nj}(\bar{z}), \qquad j = 1, 2, 3, \ldots, N \quad (7)$$

where $P_{mj}(\bar{y}) = (\bar{y})^{mj}$ and $P_{nj}(\bar{z}) = (\bar{z})^{nj}$ are the same as those for isosceles triangular ducts, except that the terms with odd exponents are retained due to lack of symmetry. Detailed steps leading to the solution are in Ref. 1. The characteristic length is equal to the base a (Fig. 2).

The circumferential average and mean Nusselt numbers when $\beta = 2.5$, 5, 10, 15, 20, 25, 30, 35, 40, and 45 deg are reported in Table 3. The definitions of the Nusselt number and the Reynolds number are the same as in the previous case; however, X differs since the value of the characteristic length a is different. For instance, when $\beta = 45$ deg in right triangular ducts, $Nu = 8.169$ and $\bar{Nu} = 12.778$ at $X = 0.0004$, whereas, for an isosceles triangular duct with $2\beta = 90$ deg, $Nu = 8.284$ and $\bar{Nu} = 12.227$ at $X = 0.0008$. The difference is 1% in Nu and 4% in $\bar{Nu} = 12.227$, and this error decreases as X increases.

Equations (2) and (3) yield a relation for calculating the bulk temperature T_b. The mean Nusselt numbers in Tables 1–3 yield the values of the bulk temperature from the relation $(T_b - T_w)/(T_o - T_w) = \exp(-4\bar{Nu}Xa^2/D_e^2)$, where T_w and T_o are wall and entering fluid temperatures.

For right triangular passages, with the included angle β tending to zero, the cross sections resemble that of parallel-plate ducts. The Nusselt number data, far away from the inlet, also reflect the same trend (note D_e is different[2]). Also as $\beta \to 0$, the results for isosceles triangular ducts with angle 2β approach that of right triangular ducts with included angle β. The accuracy of the solution, especially at small X, increases as the degree of polynomials, m_j or n_j, increases. The degree of polynomials for isosceles triangular ducts is eight corresponding to $N = 25$ terms ($m_j = 7$ and $N = 20$ for $\beta < 5$ deg), whereas it is six for right triangular ducts corresponding to $N = 28$. This is because the temperature is symmetric about the y axis (see Fig. 1), and all terms containing z to the odd powers are omitted. For this reason, one may conclude that more accurate results for right triangular ducts with small included angle may be obtained from the isosceles triangular duct solution.

References

[1]Lakshminarayanan, R., and Haji-Sheikh, A., "A Generalized Closed-Form Solution to Thermal Entrance Problems," *Heat Transfer 86*, edited by C. L. Tien, V. P. Carey, and J. K. Ferrell, Hemisphere, New York, 1986, pp. 871–876.

[2]Haji-Sheikh, A., Mashena, M., and Haji-Sheikh, M. J., "Heat Transfer Coefficient in Ducts with Constant Wall Temperature," *ASME Journal of Heat Transfer*, Vol. 105, No. 4, 1983, pp. 878–883.

[3]Haji-Sheikh, A., and Beck, J. V., "Green's Function Partitioning in Galerkin-Based Integral Solution of the Diffusion Equation," *ASME Journal of Heat Transfer*, Vol. 112, No. 1, 1990, pp. 28–34.

[4]Shah, R. K., and London, A. L., "Laminar Flow Forced Convection in Ducts," Suppl. 1, *Advances in Heat Transfer*, Academic Press, New York, 1978, p. 245.

[5]Lakshminarayanan, R., "Integral Solutions to Laminar Entrance Problems in Irregular Ducts," Ph.D. Dissertation, Univ. of Texas at Arlington, Arlington, TX 1988.

Turbulent Heat Transfer in a Square Channel with Staggered Discrete Ribs

S. C. Lau,* R. T. Kukreja,† and R. D. McMillin†
Texas A&M University, College Station, Texas 77843-3123

Received June 1, 1990; revision received Sept. 20, 1990, accepted for publication Oct. 2, 1990.

Copyright © 1991 by the American Institute of Aeronautics and Astronautics, Inc. All rights reserved.

*Associate Professor, Department of Mechanical Engineering.
†Graduate Student, Department of Mechanical Engineering.

Nomenclature

D	=	hydraulic diameter of square channel, [m]
dP/dx	=	streamwise pressure gradient in fully developed region, [N/m^3]
$\bar{f}$	=	friction factor, $(-dP/dx)D/\{2\dot{m}^2/(\rho D^4)\}$
$\dot{m}$	=	rate of mass flow of air, [kg/sec]
$\dot{q}_r''$, $\dot{q}_s''$	=	net heat fluxes on ribbed walls and smooth walls, [W/m^2]
Re_D	=	Reynolds number based on channel hydraulic diameter, $\dot{m}/(D\mu)$
$\overline{St}$	=	average Stanton number, the average of St_r and St_s
St_r	=	ribbed wall Stanton number, $\dot{q}_r'' D^2/\{\dot{m}c_p(\overline{T_{wr}} - \overline{T_b})\}$
St_s	=	smooth wall Stanton number, $\dot{q}_s'' D^2/\{\dot{m}c_p(\overline{T_{ws}} - \overline{T_b})\}$
$(\overline{T_w} - \overline{T_b})$	=	average wall/bulk temperature difference in fully developed region in channel, [K]
μ	=	dynamic viscosity of air at average bulk temperature, [N·sec/m^2]
ρ	=	density of air at average bulk temperature, [kg/m^3]

Introduction

EXPERIMENTS have been conducted to study turbulent heat transfer and friction for thermally fully developed flow of air in a square channel in which two opposite walls are roughened with staggered arrays of discrete ribs. The rib array on each roughened wall is a mirror image of that on the other (that is, corresponding ribs on the two opposite walls are parallel and aligned). The ribs in consecutive rows are turned either in the same direction or in opposite directions with respect to the wall centerline (see Fig. 1). The lengths of the discrete ribs are equal to one-half of those of the corresponding full ribs and the angled discrete ribs are cut at angles equal to the rib angles-of-attack.

The rib height-to-channel hydraulic diameter ratio is 0.0625 and the rib pitch-to-height ratio is 10. The rib angles-of-attack (α) are 45 deg, 60 deg, 90 deg, +45 deg and −45 deg in alternate rows, +60 deg and −60 deg in alternate rows, +120 deg and −120 deg in alternate rows, and +135 deg and −135 deg in alternate rows. The flow Reynolds number ranges from 10,000 to 60,000. The rib-roughened channel models the internal cooling passages in modern gas turbine airfoils. The rib configurations and the Reynolds number range are typical for turbine airfoil cooling applications.

Internal cooling passages in modern gas turbine airfoils have been investigated by researchers such as Burggraf[1] and

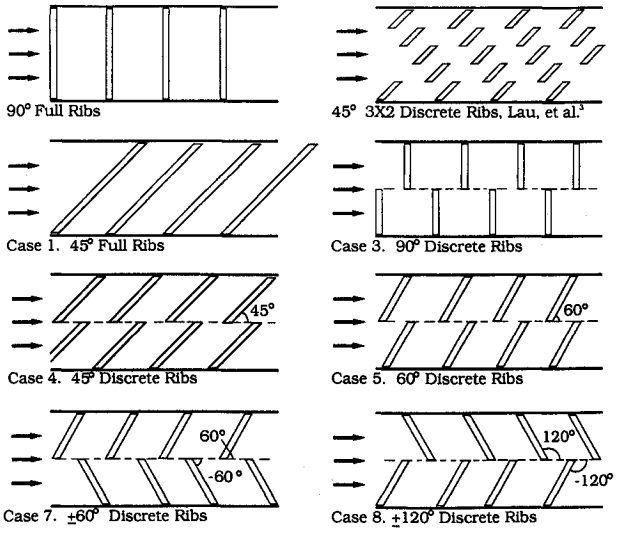

Fig. 1 Typical rib configurations.